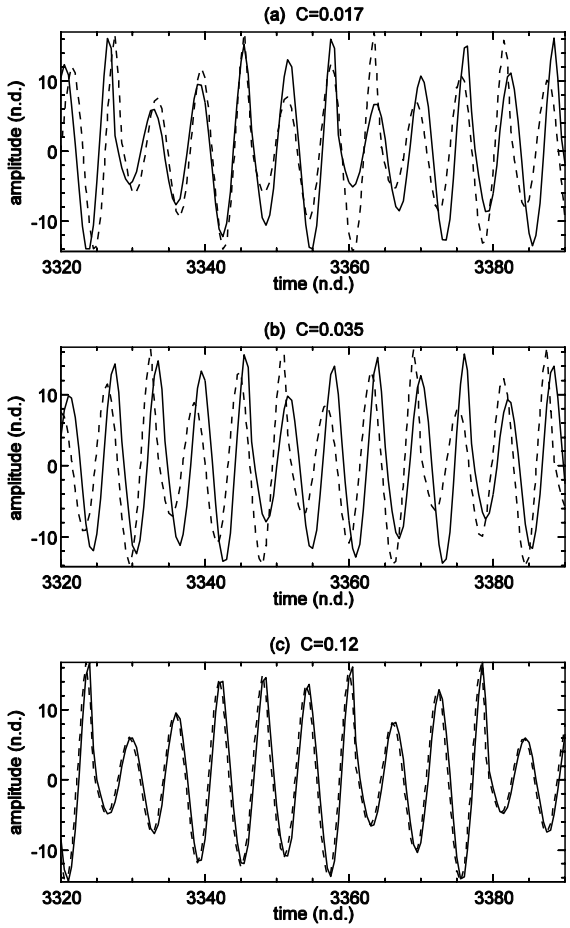

FIG. 1: The raw time series of x_1 and x_2 for two coupled Rössler oscillators; panels (a,b.c) correspond to three values of the coupling parameter C = 0.017, 0.035 and 0.120. No SSA pre-filtering is required, since the oscillations are quite regular.

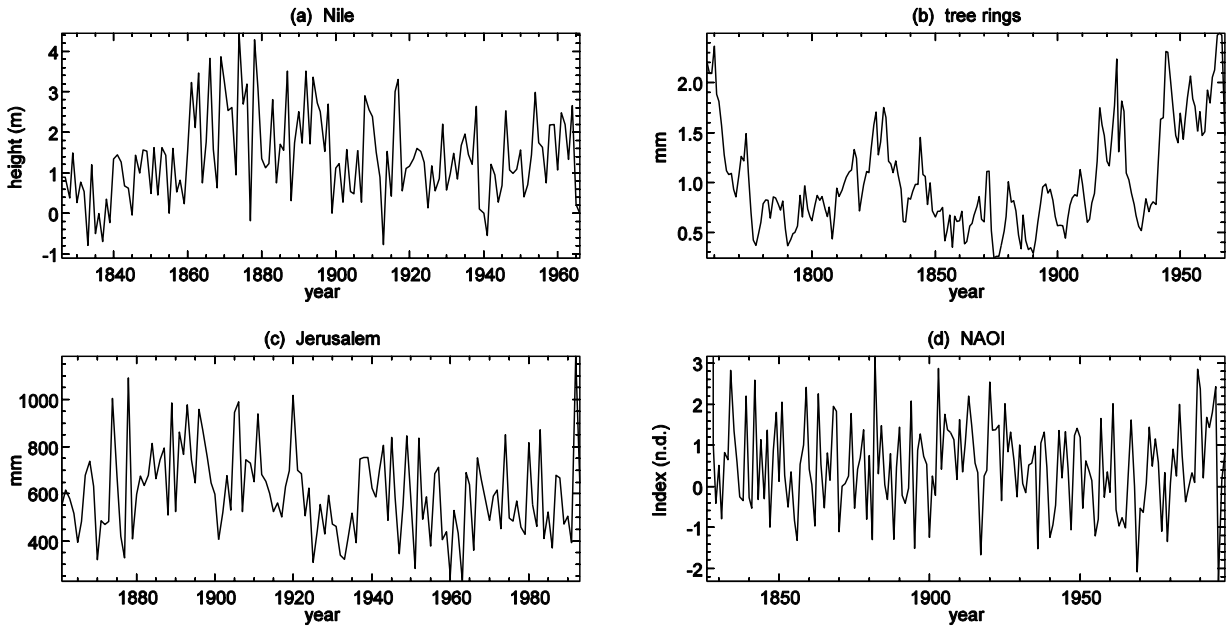

FIG. 2: The climate records used in this study. (a)–(c) Climate proxies for the Eastern Mediterranean: (a) the high-water Nile record, 1825–1972, is a proxy for the Ethiopian Plateau's climate; (b) tree-ring widths of *Quercus Infectoria* from the Golan Heights, 1757–1967; and (c) annual record of total rainfall from Jerusalem, 1861–1994. (d) Monthly values of the North Atlantic Oscillation (NAO) index, 1823–2000.

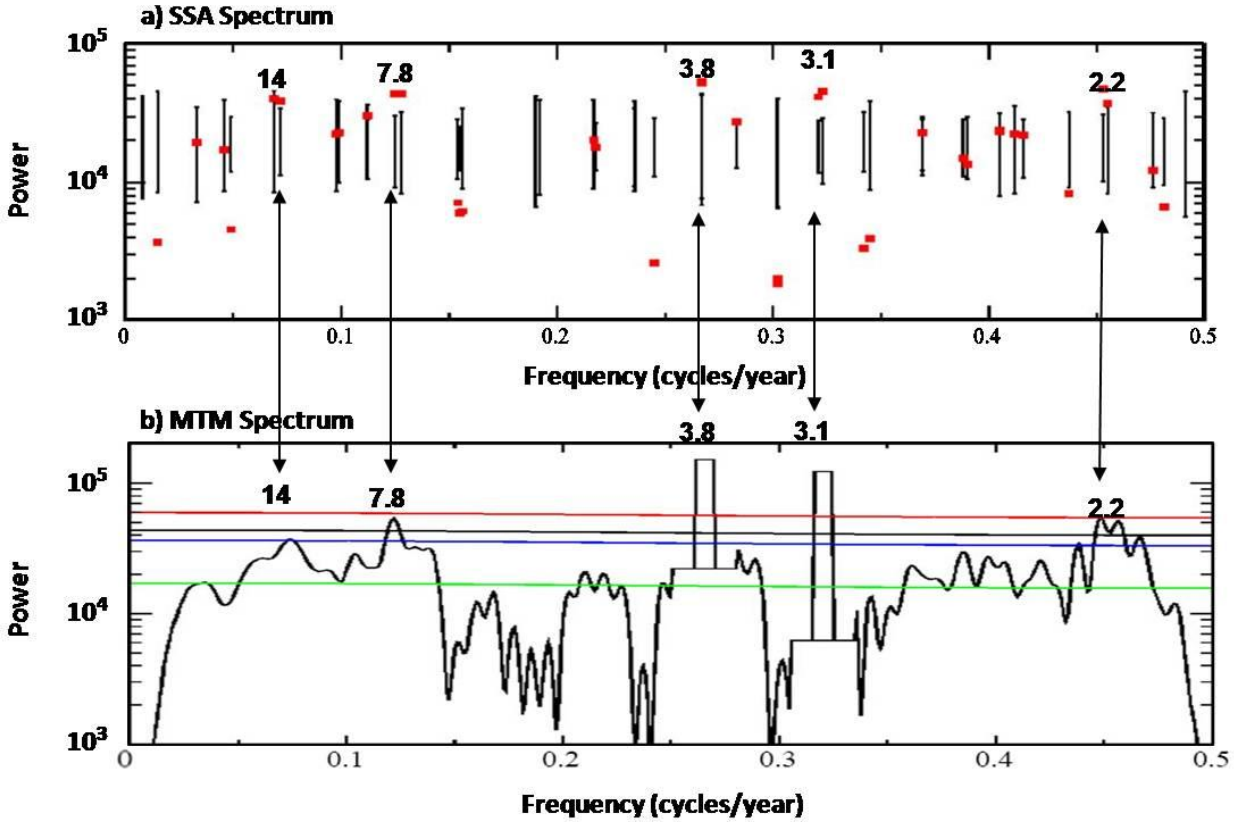

Fig. 3: Spectral analysis of the detrended time series of Jerusalem precipitation. (a) Monte Carlo SSA (MC-SSA) spectrum computed with a window width of M = 45 years; the variance of each mode in the data is in red, while lower and upper ticks on the error bars indicate the 5th and 95th percentiles of a red-noise process constructed from a surrogate data ensemble of 100 series, each with the same variance and lag-one autocorrelation as the original record. The surrogate time series (Allen and Smith, 1996) were produced by projecting the first 10 principal components of the SSA analysis onto the basis vectors of a red-noise process, with M = 45 year. (b) MTM spectrum computed with 3 tapers and spectral resolution of 0.03 cycles/year; the nearly parallel curves indicate the estimated red-noise background (lowest curve, green) and associated 50%, 90%, 95%, and 99% (highest curve, red) significance levels.

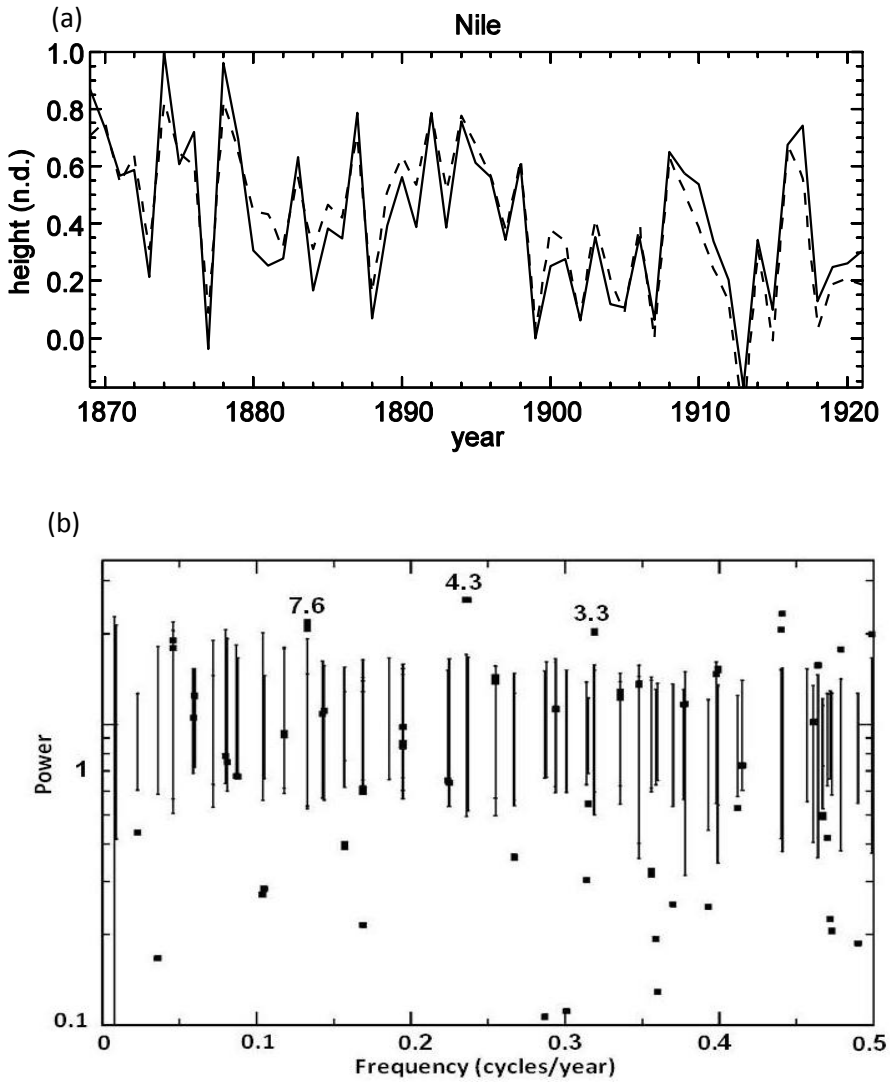

FIG. 4: The high-water Nile River records. (a) Comparison between the observed nilometer record at Rhoda Island, normalized by its maximum of 4.45 m (solid line) and the estimated high-water record — derived by linear regression, cf. Eq. (6) — from the mean annual volume flow measured at Aswan (dashed line); shown for the time interval of overlap, 1869–1922. (b) The two-channel M-SSA spectrum of the extended and detrended Nile River record (channel 1) and the NAO index for the month of August, together with a Monte Carlo significance test for the oscillations; same procedure and conventions as in Fig. 3a, except variances in black.

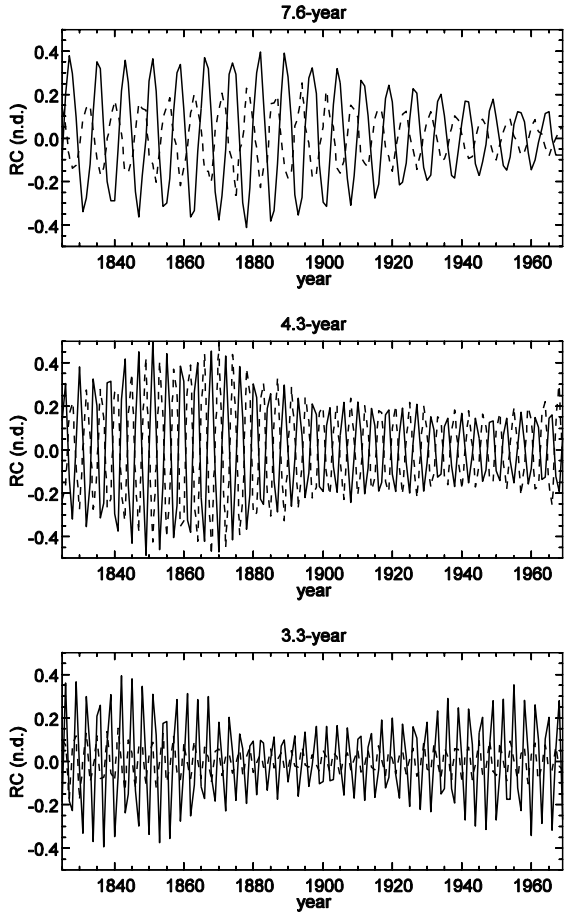

FIG. 5: The RC pairs that capture the oscillatory modes of the two-channel M-SSA for the Nile River record and the NAO index. The header of each panel is the period of the mode, in decreasing order of period length; channel 1 = Nile River (solid line), channel 2 = NAO index (dashed line).

(a)

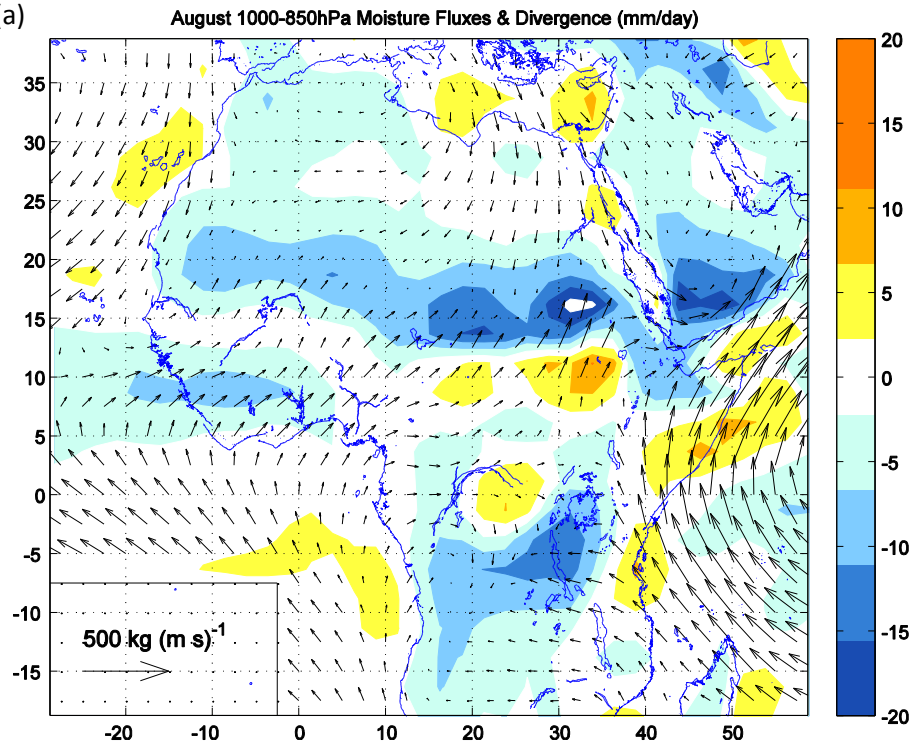

(b)

FIG. 6: Humidity supply tracks leading to the Ethiopian Plateau during summer. (a) Climatological mean map of moisture fluxes and divergence for the month of August, showing vectors of humidity fluxes averaged over the 1000–850 hPa layer, together with the flux divergence (shaded, mm/day), constructed from daily NCEP-NCAR reanalysis data, over the interval 1950–2007. (b) Schematic diagram of the three moisture tracks, labeled in the circles placed at track initiation from (1) to (3).

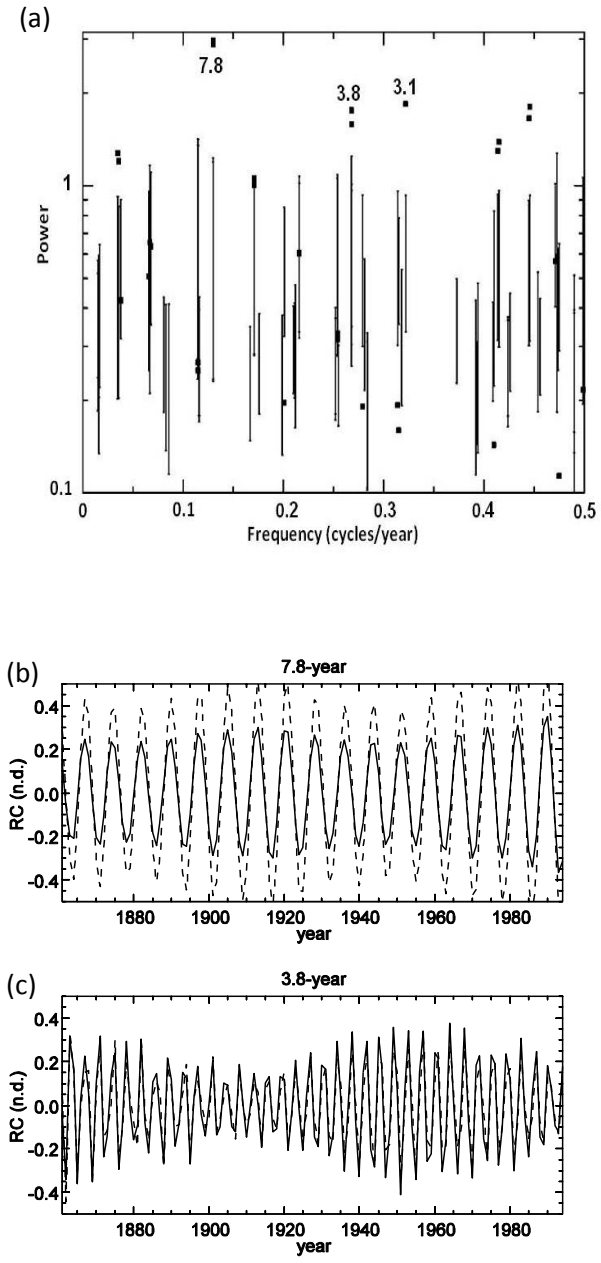

FIG. 7: Synchronization study of the NAO index (channel 1) and Jerusalem rainfall (channel 2). (a) The M-SSA spectrum of the detrended NAO index and Jerusalem precipitation data, along with the Monte Carlo significance test for the oscillatory modes. (b) The reconstruction of the 7.8-year mode of the M-SSA; NAO index (solid), Jerusalem rainfall (dashed). (c) Same as panel (b), for the 3.8-year mode.

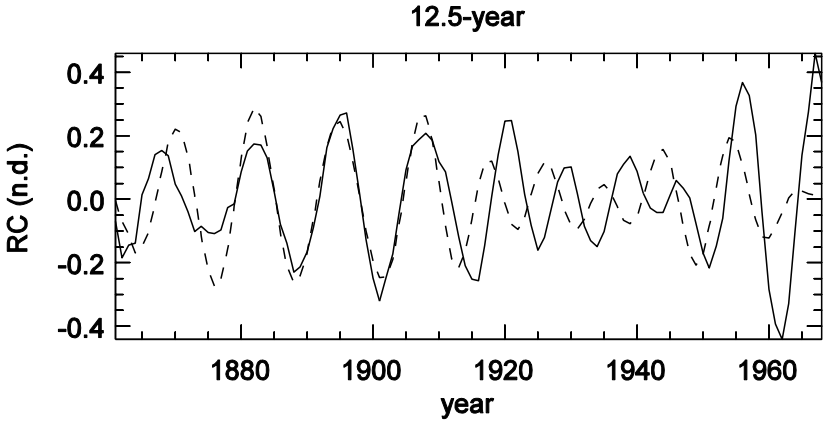

FIG. 8: The RC of the 12.5-year oscillatory mode of the joint spectra between the tree rings and Jerusalem rainfall; tree rings (solid), Jerusalem rainfall (dashed).

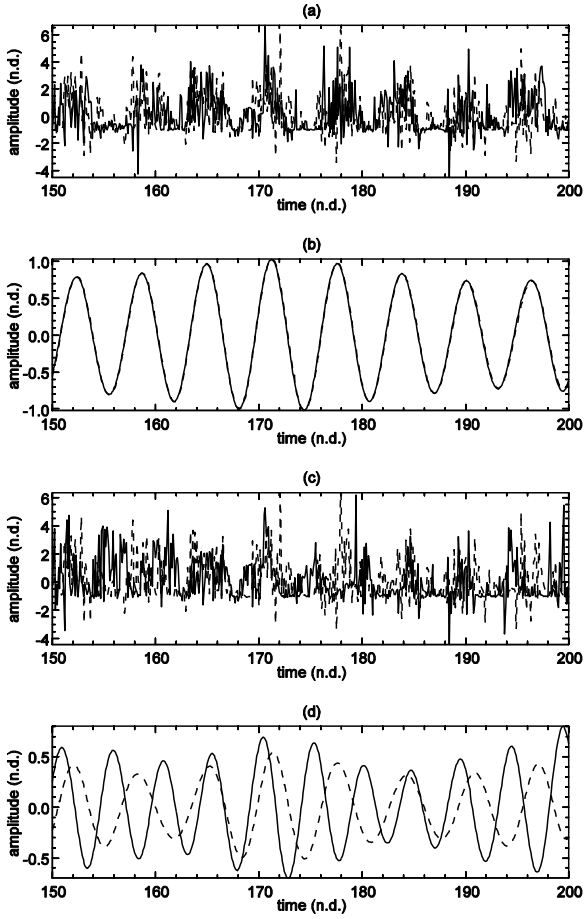

FIG. 9: Synthetic noisy time series; see Eqs. (7a, b) in appendix A. (a) Two noise-perturbed, frequency-modulated harmonic signals, $f_1(t)$ and $f_2(t)$, with the same mean period; and (b) the leading RC pair that captures the joint oscillatory mode of the two-channel SSA for $f_1(t)$ and $f_2(t)$, as given in panel (a). (c) Same as (a) but for a pair of signals that have distinct, incommensurable periods; (d) same as (b), but for the pair of signals plotted in panel (c).